Catalysis Today 148 (2009) 19–27

Contents lists available at ScienceDirect

Catalysis Today

journal homepage: www.elsevier.com/locate/cattod

Synthesis of Ti-containing mesoporous silicates from inorganic titanium sources

Huaqin Chu [a], Ying Wan [a,*], Dongyuan Zhao [b]

[a] Department of Chemistry, Shanghai Normal University, No 100 Guilin Road, Shanghai 200234, PR China
[b] Department of Chemistry and Shanghai Key Laboratory of Molecular Catalysis and Innovative Materials, Fudan University, Shanghai 200433, PR China

ARTICLE INFO

Article history:
Available online 22 May 2009

Keywords:
Mesoporous
Titanium
Inorganic source
Silicate

ABSTRACT

Titanium-containing mesoporous molecular sieves including periodic mesoporous silicas (SBA-15-type) and organosilicas (PMO-type) can be assembled by using mixed inorganic acid–base pairs ($TiCl_4$ and tetrabutyl titanate) or a single inorganic $TiCl_3$ as the titanium sources and tetraethoxysilane and/or 1,2-bis(triethoxysilyl)ethane as the silica sources and triblock copolymer as the structure-directing agent in acidic media through the hydrothermal method. Characterization using XRD, nitrogen sorption isotherms, UV–vis, FT-IR and NMR techniques reveals that the Ti-containing mesoporous materials possess ordered 2D hexagonal mesostructures, high surface areas (421–1070 m^2/g), uniform pore sizes (5.1–8.0 nm), large pore volumes (0.5–1.3 cm^3/g), and tetrahedrally incorporated titanium (IV) species in the silica network. The maximum incorporated Ti content is about 0.34 wt% for the ordered mesostructure regardless of the titania and silica sources and the initial Si/Ti ratio.

1. Introduction

Soon after the reports for mesoporous silicas synthesized by the surfactant-templating approach [1–3], Ti-containing mesoporous materials including Ti-MCM-41, Ti-MCM-48, Ti-SBA-1, Ti-SBA-15 and so on have been found to be used as versatile catalysts for the conversion of bulky molecules [4–9]. Among them, Ti-SBA-15 with a large pore size ranging from 6 to 10 nm attracts much attention. Titanium species can be incorporated into SBA-15 silica matrix either by grafting or by co-condensation method. Grafting is a post-synthesis treatment, by which metal sources incorporate on mesoporous silica from vapor deposition or impregnation and subsequent calcination [10]. Post-treatment has the problem in shaping catalysts and hence limits the application in industry because calcined mesoporous silica powders lacking surface hydroxyl groups are normally used as a matrix. By comparison, titanium can be directly introduced into the silica framework by one-step condensation [11]. Shaping can be easily carried out on the basis of the as-made materials which have plenty of hydroxyl groups on the surface. One-step synthesis also shows the advantage in the possibly uniform distribution of titanium species and the avoidance of pore blockage [12]. The co-condensation synthesis involves the cooperative assembly between organic surfactant templates and inorganic precursors. Besides interaction between organic and inorganic species, the interaction inside the inorganic species themselves should be considered [13,14]. In the synthesis of Ti-containing mesoporous silicas, the hydrolysis and condensation of titania should be fully considered because of much faster rates than those of silica [12,13]. Several methods have been used to reduce the hydrolysis and condensation rates of Ti precursors or improve the hydrolysis rate of silica sources [5]. Expensive organic titanium sources are normally applied. For example, the initial reports on mesoporous titanium-containing mesoporous silicas used chemically modified Ti-alkoxide to control over the rate of hydrolysis of the metal precursor [15,16]. Melero et al. prepared Ti-containing mesoporous silica by using titanocene dichloride as a titanium source [13]. Titanium isopropoxide was used to prepare titanium-modified hybrid periodic mesoporous organosilicas by Cho et al. [17].

The catalytic performance of hybrid mesoporous silicas is strongly related to the surface chemical characters, especially hydrophobicity [18]. A high hydrophobicity of the solid surface can lead to a high catalytic performance [19,20]. Periodic mesoporous organosilicas (PMOs) have been reported to improve hydrophobicity, and therefore, be very efficient in catalysis [21]. However, the synthesis is mainly carried out in the basic conditions by using cationic surfactant as a structure-directing agent (SDA). The pore size is limited to 3.3 nm [22].

Here, we report for the first time the synthesis of Ti-containing mesoporous silica by using mixed inorganic "acid–base pairs" titanium sources, namely acidic $TiCl_4$ and basic counterpart $Ti(OC_4H_7)_4$ which can self-generate a proper acidic media for the sol–gel process via the triblock-copolymer templating co-condensation approach under acidic conditions. The self-adjustment of the

* Corresponding author. Tel.: +86 21 6432 2516; fax: +86 21 6432 2272.
E-mail address: ywan@shnu.edu.cn (Y. Wan).

0920-5861/$ – see front matter © 2009 Elsevier B.V. All rights reserved.
doi:10.1016/j.cattod.2009.03.008

hydrolysis and condensation of titanium sources favors the surfactant-templating assembly and the gelation of inorganic species [23]. For comparison, the inorganic source of $TiCl_3$ which has a low hydrolysis rate was also used in the synthesis. To improve pore surface hydrophobicity, Ti-PMOs are further synthesized by using triblock copolymer as a template and inorganic $TiCl_3$ as a single titanium source. The obtained Ti-containing mesoporous silicates have highly ordered 2D hexagonal structure, uniform pore sizes (5.1–8.0 nm), high surface areas (421–1070 m^2/g), large pore volumes (0.5–1.3 cm^3/g) and tetrahedrally coordinated titanium sites.

2. Experimental

2.1. Materials

Poly(ethylene oxide)-*block*-poly(propylene oxide)-*block*-poly (ethylene oxide) triblock copolymer Pluronic P123 ($EO_{20}PO_{70}EO_{20}$, M_w = 5,800) and 1,2-bis(triethoxysilyl)ethane [$(CH_3CH_2O)_3SiCH_2CH_2Si(OCH_2CH_3)_3$, BTESE, 96%], were obtained from Aldrich Chemical Company. Tetraethoxysilane (TEOS, 98%), titanium tetrachloride ($TiCl_4$, 98%), tetrabutyl titanate (TBOT, 98%), titanium trichloride ($TiCl_3$, 15% solution in hydrochloric acid solution), hydrogen chloride (HCl, 36.0–38.0%), and isopropanol (C_3H_7OH, 99.5%) were obtained from Shanghai Chemical Company. All chemicals were used as received without any further purification. Water used in all syntheses was distilled and deionized.

2.2. Synthesis of Ti-containing mesoporous molecular sieves

2.2.1. $TiCl_3$ as a single inorganic titanium source for the synthesis of Ti(S)-SBA

The synthesis for Ti(S)-SBA is similar to that for well-reported SBA-15 silica by using triblock copolymer as a structure-directing agent and TEOS as a silica source under acidic conditions except for the addition of titanium source $TiCl_3$. The Ti(S)-SBA materials were synthesized by using titanium trichloride as a single titanium source, TEOS as a silica source, and triblock copolymer P123 as a structure-directing agent. A typical synthesis was: 2.0 g of P123 were dissolved in 30 ml of 1.0 M HCl and 15 ml H_2O at 40 °C. Then 3.95 g (19 mmol) of TEOS were added to the clear solution under vigorous stirring for 2 h to form a mixture solution. To it, 0.15 g (1 mmol) of $TiCl_3$ were slowly added with stirring. After 22 h, a gel of the following molar composition was obtained: xSiO$_2$:yTiO$_2$:0.017P123:41.7H_2O ($x + y = 1$), wherein the ratio of x/y, ranging from 100 to 5, could be regulated by controlling the ratio of TEOS to $TiCl_3$. The gel was transferred into an autoclave with a polytetrafluoroethylene (PTFE) insert and subjected to a hydrothermal treatment under autogenous pressure at 100 °C for 24 h. The solid products were recovered by filtration, washing with deionized water and drying at 80 °C for 12 h under vacuum. The resulting powders were calcined at 450 °C for 10 h in air to remove the surfactant. The obtained materials are denoted as Ti(Sx/y)-SBA, wherein S represents the single inorganic titanium source and x/y is the Si/Ti ratio in the initial synthesis batch.

2.2.2. $TiCl_4$ and TBOT as the mixed inorganic titanium sources for the synthesis of Ti(M)-SBA

Ti(M)-SBA were synthesized by using $TiCl_4$ and TBOT as mixed titanium sources, TEOS as a silica source, and triblock copolymer P123 as a structure-directing agent. A typical synthesis was: 2.0 g of P123 were dissolved in 30 ml of 1.0 M HCl and 15 ml H_2O at 40 °C. Then 3.95 g (19 mmol) of TEOS were added to the clear solution under vigorous stirring for 2 h to form the mixture A. The mixture B constituted by 0.057 g (0.3 mmol) of $TiCl_4$, 0.20 g (0.7 mmol) of TBOT and 8.0 ml of isopropanol were vigorously stirred at 40 °C for 0.5 h. The mixture B were then slowly added to the mixture A with stirring. After 22 h, a gel of the following molar composition was obtained: xSiO$_2$:yTiO$_2$:0.017P123:41.7H_2O ($x + y = 1$), wherein the ratio of x/y, ranging from 100 to 8.5, could be regulated by controlling the ratio of TEOS to the mixture of $TiCl_4$ and TBOT. The gel was heated to 80 °C to remove isopropanol, and then transferred into an autoclave. The subsequent treatment was the same as that for Ti(S)-SBA. The obtained materials are denoted as Ti(Mx/y)-SBA, wherein M represents the use of mixed titanium source.

2.2.3. $TiCl_3$ as a single inorganic titanium source for the synthesis of organic–inorganic hybrid Ti(S)-PMO

The synthesis of organic–inorganic hybrid Ti-containing PMOs involved the use of $TiCl_3$, TEOS, BTESE and Pluronic P123 under acidic conditions, which was similar to the above synthesis for Ti(S)-SBA. A typical synthesis is as follows. To the clear solution containing 2.0 g of P123, 30 ml of 1.0 M HCl and 15 ml H_2O, 3.6 g (17.1 mmol) of TEOS were added at 40 °C under vigorous stirring. After 1 h, 0.70 g (1.9 mmol) of BTESE were dropped into it and the mixture were stirred for another 1 h. Then 0.15 g (1 mmol) of $TiCl_3$ was slowly added to the mixture. A gel was obtained after 22 h, and then transferred to an autoclave with a polytetrafluoroethylene (PTFE) insert for the hydrothermal treatment. The hydrothermal treatment and time was 100 °C and 24 h, respectively. The products were filtered, washed and dried according to the above procedure. Solvent extraction was adopted to remove the template. 1.5 g of as-made material was mixed with 500 ml of ethanol with reflux under stirring at 80 °C for 24 h. The solids were then recovered by filtration, washing and drying at 80 °C for 12 h under vacuum, and named as Ti(Sx/y)-PMOs, wherein x/y represents the Si/Ti molar ratio in the initial solution, and S means the use of a single inorganic source.

2.3. Characterization

N_2 adsorption–desorption isotherms were measured at 77 K with a Quantachrome NOVA 4000e analyzer. Before measurements, the samples were degassed in a vacuum at 120 °C for at least 6 h. The Brunauer–Emmett–Teller (BET) method was utilized to calculate the specific surface areas (S_{BET}). By using the Barett–Joyner–Halenda (BJH) model, the pore volumes and pore size distributions were derived from the adsorption branches of isotherms, and the total pore volumes (V_t) were estimated from the adsorbed amount at a relative pressure p/p_0 of 0.99. The micropore volume (V_m^{micro}) and micropore surface area (S_{BET}^{micro}) were calculated from the V–t plot method. The t values were calculated as a function of the relative pressure using the de Boer equation, $t/Å = [13.99/(\log(p_0/p) + 0.0340)]^{1/2}$. V_m was obtained using the equation $V_m/cm^3 = 0.001547I$, where I represents the Y intercept in the V–t plot. Scanning electron micrographs (SEM) were taken on a XL 30 philips 20 kV. Fourier transform infrared (FT-IR) spectra were collected on a Nicolet Fourier spectrophotometer, using KBr pellets of the solid samples. The X-ray diffraction (XRD) measurements were taken on a Rigaku Dmax-3C diffractometer using Cu Kα radiation (40 kV, 30 mA, λ = 0.15408 nm). The d-spacing values were calculated by the formula $d = \lambda/2\sin\theta$, and the unit cell parameters were calculated from the formula $a_0 = 2d_{10}/\sqrt{3}$. UV–vis diffuse reflectance spectra were recorded on a Shimadzu 2401PC UV–vis spectrophotometer with an integrating sphere attachment using $BaSO_4$ as the background standard. ^{13}C CP MAS NMR spectra were obtained at 75.4 and 59.6 MHz for samples (100–200 mg) contained in 7 mm zirconia rotors undergoing magic angle spinning (at 5 kHz) on a Bruker ASX-300 spectrometer. ^{13}C shift was referenced externally to samples of adamantane (39.5 ppm) and tetrakis

(trimethylsilyl) silane (−9.8 ppm), respectively. ^{13}C spectra were collected with 70° rf pulses (4 μs), 5 s delay and ca. 6000 scans. The Ti content was determined by X-ray Fluorescene (Rigaku Mini-prime) using H_3BO_3 pellets of the solid samples.

3. Results and discussion

3.1. Mesostructure

Ti-containing mesoporous silicate catalysts have been synthesized by assembling silica source, inorganic titanium species and triblock copolymer P123 under acidic conditions. Fig. 1a shows the small-angle XRD patterns of Ti(M)-SBA by using $TiCl_4$ and TBOT as mixed inorganic titanium sources and TEOS as a silica source. The catalysts with the Si/Ti ratio of 20 and 12.5 in the initial solution (Ti(M20)-SBA and Ti(M12.5)-SBA) exhibit one strong and two weak diffraction peaks, which can be indexed to the 10, 11 and 20 planes belonging to the ordered 2D hexagonal mesostructure. The titanium content shows a negligible effect on the cell parameter that is calculated to be 10.5 nm. The wide-angle XRD patterns (Supporting Information, SI Fig. S1a) show only one diffused diffraction peak at about 24°, suggesting the amorphous substance. No diffraction peaks attributed to crystalline titania are found. Although the formation of well-distributed, nano-sized titania in the framework cannot be completely excluded, this phenomenon, at least partially, implies that titanium has been incorporated into the silica matrix. To the best our knowledge, this is the first report for the synthesis of ordered Ti-containing meosporous silica by using inorganic $TiCl_4$ and TBOT as mixed titanium sources and triblock copolymer as a template under conventional acidic hydrothermal conditions. It should be noted that the titanium content in the final product is far less than that in the initial solution. The Si/Ti ratio in the final solids is 387 and 221 for Ti(M20)-SBA and Ti(M12.5)-SBA, respectively. The main reason is that Ti–O–Si bonds can be easily dissociated under the acidic conditions [13,24]. Most titanium species are dissolved in mother solution instead of involvement in the silica framework. If the Si/Ti ratio reduces to 10 and 8.5, the small-angle XRD patterns for Ti(M10)-SBA and Ti(M8.5)-SBA get less resolved. Only one peak at 2θ of about 1.1° can be observed and the diffraction peaks in the range of 1.5–3° disappear, suggesting that the mesostructure becomes less ordered. Relatively low Si/Ti ratios of 56 and 40 are detected for the final molecular sieves. On comparison with Ti(M)-SBA with high Si/Ti ratios, the wide-angle XRD pattern for Ti(M10)-SBA displays several additional diffraction peaks, which can be assigned to anatase (SI Fig. S1a). The diffraction peaks are wide, implying the tiny titania particles. This result indicates that not all titanium incorporate into silica matrix and a large amount of anatase are formed in the final solids with the increase of titanium content. The generation of anatase may explain the fact that the Si/Ti ratio distinctly increase in the Ti(M10)-SBA on comparison with that of Ti(M12.5)-SBA despite of the close Si/Ti ratio. The less resolved XRD patterns for Ti(M)-SBA materials with a low Si/Ti ratio may be related to the presence of tiny anatase particles and structural defect after incorporation of more titanium into silica framework. These phenomena reflect that the ordered mesostructure can only be obtained with a titanium content of about 0.36 wt% by using blending $TiCl_4$ and TBOT as mixed titanium sources. The increase in the titanium content may lead to the destruction of mesostructure.

N_2 sorption isotherms for Ti(M)-SBA materials with different Si/Ti ratios show typical type-IV curves with a clear condensation step at middle relative pressures, characteristic of the mesoporous silica SBA-15 material (Fig. 2a). However, different from a pure silica SBA-15, titanium-containing mesoporous silica materials do not give a good H1-type hysteresis loop, implying that the pore channels are not ideally cylindrical. This phenomenon has also been observed in the metal-substituted mesoporous silicates, which is assigned to the different condensation on pore walls between hybrid species and silica [25]. The Ti(M20)-SBA and Ti(M12.5)-SBA materials shows uniform pore-size distribution (~6 nm), high surface areas (~1000 m^2/g) and large pore volumes

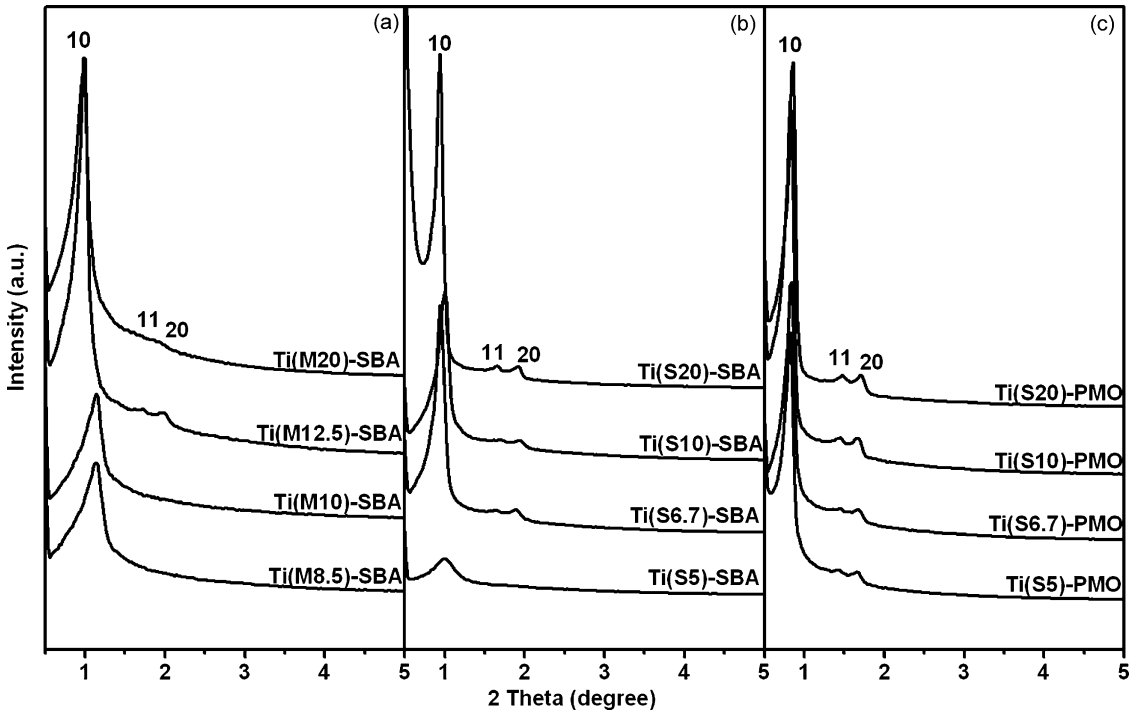

Fig. 1. Small-angle XRD patterns of Ti-containing mesoporous silicas prepared from mixed $TiCl_4$ and TBOT titanium sources (Ti(M)-SBA) (a) or a single $TiCl_3$ titanium source (Ti(S)-SBA) (b), and Ti-containing periodic mesoporous organosilicas prepared from a single $TiCl_3$ titanium source (Ti(S)-PMO) (c) via the triblock-copolymer templating approach. The number in each sample denotes the Si/Ti ratio in the initial synthesis solution.

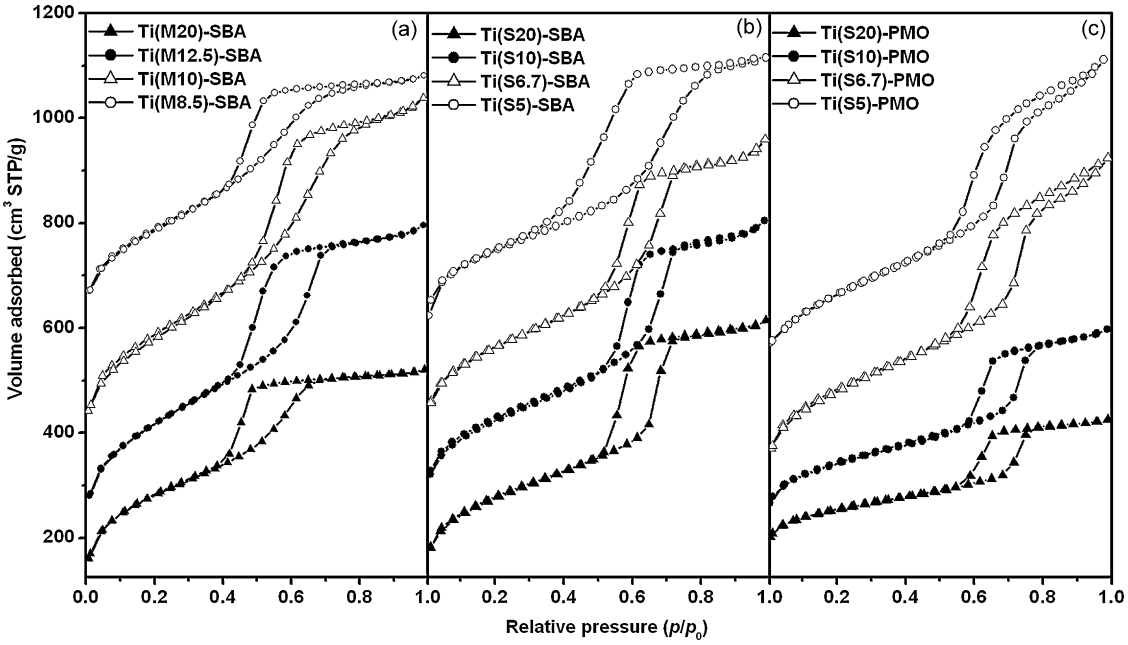

Fig. 2. N_2 sorption isotherms for Ti-containing mesoporous molecular sieves via the triblock-copolymer templating co-condensation approach: Ti(M)-SBA prepared using mixed inorganic $TiCl_4$ and TBOT as titanium sources and TEOS as a silica source (a); Ti(S)-SBA prepared using $TiCl_3$ as a single inorganic titanium source and TEOS as a silica source (b); Ti(S)-PMO prepared using inorganic $TiCl_3$ as a single titanium source and TEOS and BTESE as mixed silica sources (c). The isotherms of Ti(M12.5)-SBA, Ti(M10)-SBA, Ti(M8.5)-SBA are offset vertically by 120, 300 and 520 cm^3/g. The isotherms in (b) are offset vertically by 20, 100, 130 and 380 cm^3/g, for the sample with the Si/Ti ratio of 20, 10, 6.7 and 5, respectively. The isotherms of Ti(S20)-PMO, Ti(S10)-PMO, Ti(S6.7)-PMO and Ti(S5)-PMO in (c), are offset vertically by 40, 100, 260 and 200 cm^3/g, respectively.

($\sim$1.0 cm^3/g). When the Si/Ti ratio reduces to 8.5, a type H4 hysteresis loop is observed. This kind of loop is often associated with narrow slit pores from non-rigid aggregates of plane-like particles, or pores in the micropore region [26]. On the analysis of *V–t* plots, micropores contribute below 10% to the total pore surface areas and volumes (Table 1 and SI Fig. S2). As a result, nanorigid aggregates of silica or anatase may be responsible for the type H4 loop. With the increase of the titanium content, the pore-size distribution becomes non-uniform (Fig. 3a). These results are in accordance with the XRD patterns, which reflect disordered mesostructure for the Ti-containing mesoporous silicates with Si/Ti ratios of 10 and 8.5.

By comparison, $TiCl_4$ or TBOT is also used as a single titanium precursor. The Si/Ti ratio is 12.5 in the synthesis batch. However, disordered materials are produced after the hydrothermal treatment as evidenced by only an extremely low diffraction peak in the small-angle XRD patterns (Fig. 4a). In fact, white precipitation is formed once the addition of the solution composed of $TiCl_4$ (or TBOT) and isopropanol, indicating that macroscopic separation may occur at the beginning of the synthesis. This phenomenon is possibly related to the much higher hydrolysis and condensation rates of these inorganic titanium sources than TEOS under the conventional acidic hydrothermal conditions. Moreover, $TiCl_4$ or $Ti(OC_4H_9)_4$ catalyzes silanol condensation, promoting homocondensation of the silicate species rather than uniform incorporation of Ti at the molecular level [27]. Crystalline anatase is the major product after calcination (Fig. 4b). The weak diffraction peaks may come from the mesostructured silica assembles after hydrothermal reaction.

Therefore, the successful synthesis of ordered Ti-containing mesoporous silicates can be attributed to the choice of the "acid–base pairs" as titanium precursors, i.e. $TiCl_4$ and $Ti(OC_4H_9)_4$. Inorganic metallic or nonmetallic chlorides are considered as strong "acid" since a large amount of acid is generated during the alcoholysis process, and metallic alkoxides are assigned to base because acid substances are seldom generated. The "acid–base pairs" have been verified to be a facile and reproducible method for preparing ordered mesoporous titania solids, because of

Table 1
Structural, textural and catalytic properties of Ti-containing mesoporous silicates.

Sample	Si/Ti ratio[a]	Si/Ti ratio[b]	Ti content (wt%)[c]	a_0 (nm)	S_{BET} (m^2/g)	V_t (cm^3/g)	D_p (nm)	S_{BET}^{micro} (m^2/g)	V_p^{micro} (cm^3/g)
Ti(M20)-SBA	20	387	0.21	10.5	986	0.81	5.1	238	0.106
Ti(M12.5)-SBA	12.5	221	0.36	10.4	1070	1.1	6.3	90	0.030
Ti(M10)-SBA	10	56	1.4	9.0	1037	1.1	5.7	77	0.023
Ti(M8.5)-SBA	8.5	40	1.9	9.0	1349	1.2	4.5	93	0.035
Ti(S20)-SBA	20	440	0.18	10.8	868	0.93	6.3	149	0.062
Ti(S10)-SBA	10	383	0.20	10.4	908	1.0	6.3	125	0.050
Ti(S6.7)-SBA	6.7	235	0.34	10.8	961	1.1	6.3	136	0.056
Ti(S5)-SBA	5	21	3.6	10.3	876	0.99	6.3	158	0.066
Ti(S20)-PMO	20	365	0.21	11.9	421	0.5	8.0	24	0.006
Ti(S10)-PMO	10	244	0.33	12.1	598	0.7	8.0	0	0
Ti(S6.7)-PMO	6.7	232	0.34	12.3	928	1.2	8.0	0	0
Ti(S5)-PMO	5	254	0.31	12.9	980	1.3	7.1	0	0

[a] The Si/Ti molar ratio in the initial synthesis batch.
[b] The Si/Ti ratio in the final solid.
[c] The calculation of the titanium content is based on the assumption that the final solids are composed of silica and titania.

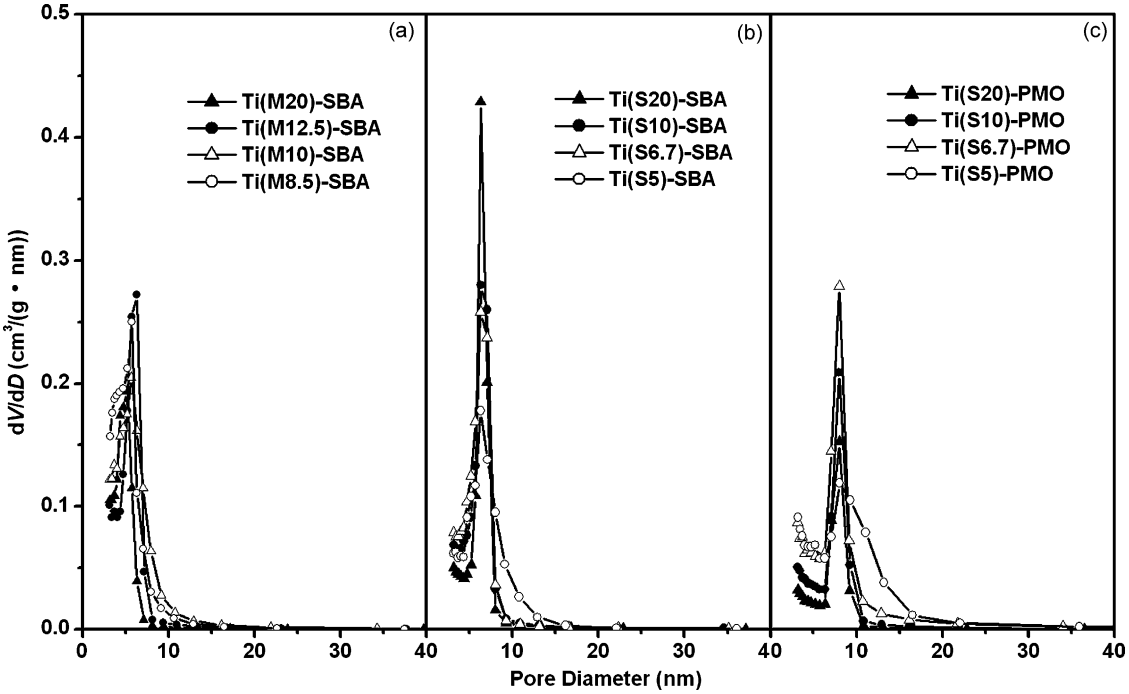

Fig. 3. Pore-size distribution curves for Ti-containing mesoporous molecular sieves via the triblock-copolymer templating co-condensation approach: Ti(M)-SBA from mixed inorganic titanium sources of $TiCl_4$ and TBOT and a silica source of TEOS (a); Ti(S)-SBA from a single inorganic titanium source of $TiCl_3$ and a silica source of TEOS (b); Ti(S)-PMO from a single inorganic titanium source of $TiCl_3$ and mixed silica sources of TEOS and BTESE (c). The number in each sample denotes the Si/Ti ratio in the initial synthesis batch.

self-adjusted acidity during the sol–gel process [23,27]. In the present case, $TiCl_4$ and $Ti(OC_4H_9)_4$ firstly alcoholyze in isopropanol. At that time, $TiCl_{4-x}(OC_3H_7)_x$ and $Ti(OC_4H_9)_{4-y}(OC_3H_7)_y$ ($x \geq 1$; $y \geq 1$) are formed without condensation to Ti–O–Ti bonds (at least partially) [23]. The pre-hydrolyzed silicate species of, for example, $(OR)_3Si–OH$ can react with titanium species of, for example, $TiX_3(OC_3H_7)$ to form $(OC_2H_5)_3Si–O–TiX_3$ (X = Cl and $–OC_4H_9$) via the heterocondensation reaction. Simultaneously, the formed proper acidic medium during the alcoholysis of $TiCl_4$ and $Ti(OC_4H_9)_4$ favors the inorganic–organic assembly and the heterocondensation reaction of inorganic precursors. Therefore, silicon and titanium species assemble around the triblock copolymer aggregates, and cross-link and condense to form mesostructured hybrids, avoiding the precipitation of titanium hydroxide. But it should be noted that the incorporation of alcoholyzed titanium species into the silica matrix is limited to a certain range. Once the titanium content is over-high, the aggregation of titania may occur, leading to the reduced regularity. This speculation can be confirmed by the UV–vis spectra which will be discussed in the following section. On the contrary, the over-fast hydrolysis and condensation rates of a single titanium source $TiCl_4$ or $Ti(OC_4H_9)_4$ and the catalysis role of $TiCl_4$ or $Ti(OC_4H_9)_4$ for homocondensation of the silicate species may lead to the formation of precipitation of titanium species instead of interacting with silica species. A large amount of crystalline anatase is formed after calcination.

Another factor is the heating step before hydrothermal treatment. The reactant mixture of Ti(M12.5)-SBA were also

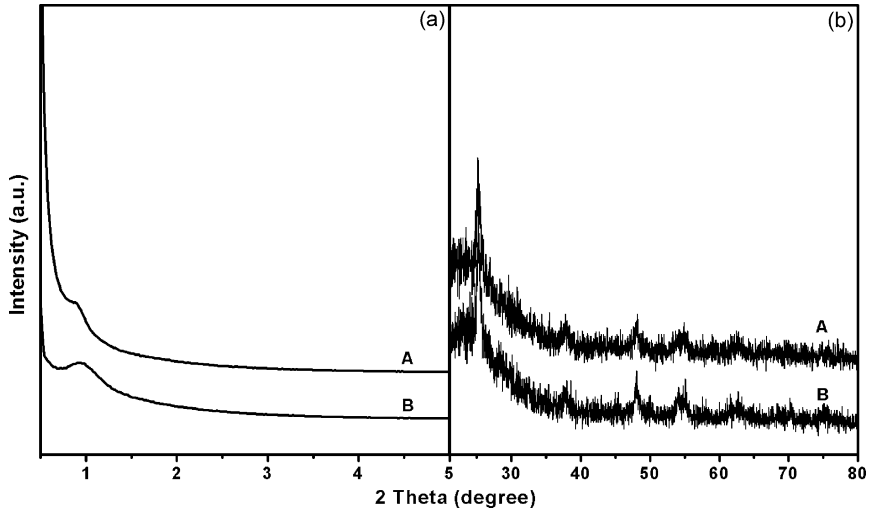

Fig. 4. Small-angle (a) wide-angle (b) XRD patterns of Ti-containing mesoporous silicas prepared using TEOS as a silica source, triblock copolymer P123 as a structure-directing agent, and $TiCl_4$ (A) or TBOT (B) as a single titanium source. The Si/Ti mole ratio in each synthesis batch is fixed at 12.5.

directly subjected to hydrothermal treatment without heating at 80 °C. The small-angle XRD pattern only shows one wide diffraction peak, indicative of disordered products (SI Fig. S3). Isopropanol is used to dissolve $TiCl_4$ and $Ti(OC_4H_9)_4$ during the synthesis. It is well known that solubilization of impurities in micelles causes changes in the surface energy, and lyophilic organics can aid or oppose the formation of micelles [28,29]. At high concentrations, short-chain alcohols can enhance the solubility of nonionic surfactants, thus suppressing micellization and raising critical micelle concentration (CMC) values. The assembly of block copolymers is inhibited. On the other hand, the presence of a large amount of isopropanol may change the hydrothermal self-generous pressure. Therefore, a heating step at 80 °C is carried out to remove alcohols.

The pre-hydrolysis of TEOS under acidic conditions is also a key factor for the synthesis. The XRD results reveal that disordered materials were obtained under conventional conditions, where the solution of $TiCl_4$ and $Ti(OC_4H_9)_4$ and TEOS were hydrolyzed simultaneously in the presence of P123 and aqueous HCl (data not sown here). Here, the titanium species is added into the synthesis batch containing pre-hydrolyzed TEOS and triblock copolymer. Then the condensation rates for silica and titania species can match well with each other to form hybrid titanium-incorporated silica. The amine-group-functionalized SBA-15 materials have also been found to be prepared by co-condensation of a pre-hydrolyzed TEOS and 3-aminopropyltriethoxysilane under acidic triblock-copolymer templating conditions [14,30]. 3-Aminopropyltriethoxysilane can also catalyze the homocondensation of TEOS. Therefore, the heterocondensation can only occur between pre-hydrolyzed inorganic silicate species and organic silicate species. At that time, the mesostructured inorganic–organic composites are formed because of the heterocondensation between the two silica sources and interaction of hydrolyzed and condensed silica species with triblock copolymer P123.

In comparison with $TiCl_4$ and TBOT, $TiCl_3$ has a relatively slow hydrolysis rate. Fig. 1b shows the small-angle XRD patterns for the Ti(S)-SBA materials by using $TiCl_3$ as a single titanium source. Different from the materials prepared with a single $TiCl_4$ or TBOT source, Ti(S)-SBA shows well-resolved XRD patterns assigned to the ordered mesostructure with the *p6mm* symmetry when the Si/Ti ratio in the initial solution exceeds 6.7. The cell parameters (about 10.8 nm) are close to that for Ti(M)-SBA with an ordered mesostructure and do not distinctly change with the titanium content. No distinct diffraction peaks belonging to anatase in the wide-angle XRD patterns can be observed for the Ti(S)-SBA materials with a Si/Ti ratio above 6.7. The XRD pattern for Ti(S5)-SBA shows only one wide diffraction peak, indicative of disordered mesostructure. Simultaneously, anatase is formed in the product as evidenced by the diffraction peaks at 2θ of 25, 39, 48 and 54°. The results are similar to those for Ti(M)-SBA prepared by mixed inorganic sources. The increase of titanium content in the synthesis batch leads to the destruction of mesostructure and formation of anatase. The Si/Ti ratio in the final solids is 440, 383, 235, and 21, for Ti(S20)-SBA, Ti(S10)-SBA, Ti(S6.7)-SBA and Ti(S5)-SBA, respectively. The formation of a large amount of anatase in the product when over-high titanium precursors are added in the synthesis batch accompanies with the distinct increase in Si/Ti ratio and destruction of mesostructure. It is interesting that the highest titanium content (0.34 wt%) for the maintenance of the ordered mesostructure prepared using a single inorganic $TiCl_3$ precursor is similar to that in materials prepared with mixed $TiCl_4$ and TBOT sources. Typical type-IV N_2 sorption isotherms with a H1 type hysteresis loop are observed for Ti(S)-SBA with a titanium content below 0.34 wt% (Fig. 2b), indicating the presence of perfect uniform cylindrical pores. The parallelogram loop becomes distorted when the titanium content increases to 3.6 wt%, suggesting the distortion of pores. The pore-size distribution curve for Ti(S5)-SBA is wider than that for the sample with a low titanium content (Fig. 3b).

Periodic mesoporous organosilicas (PMOs) have been reported to be an important member in the mesoporous family due to the fact that the unique hybrid inorganic–organic framework shares the advantages of rigid inorganic matrix and the functionality of organic components [31–33]. Here, the inorganic titanium source $TiCl_3$ was also used to synthesize hybrid organic–inorganic mesoporous materials (Ti(S)-PMO). The Si/Ti ratio in the synthesis batch ranges from 20 to 5, similar to that in Ti(S)-SBA materials. The small-angle XRD patterns (Fig. 1c) show that all Ti(S)-PMO materials have the ordered 2D hexagonal mesostructure with the *p6mm* symmetry and the cell parameter of 12.3 nm; and the wide-angle XRD patterns show only one diffused diffraction peak assigned to amorphous substance (SI Fig. S1c). The titanium content in the final solids is in the range from 0.21 to 0.34 wt%. Ti(S10)-PMO, Ti(S6.7)-PMO and Ti(S5)-PMO have the similar titanium content despite of the large difference in the initial batch. These results are different from the above Ti-SBA materials, which exhibit a reduced regularity and an increasing titanium content with the decrease of the Si/Ti ratio in the synthesis batch. The possible reason is the inherent hydrophobicity of BTESE which influences the hydrolysis and condensation of silica species. The hydrolysis and condensation rates for titania and silica sources may match well with each other, inhibiting the occurrence of titania aggregates, even if the Si/Ti ratio is low in the synthesis batch. It can be seen that the maximum titanium content in the silica framework is about 0.34 wt% under the acidic conditions regardless of the adding amount of titanium content and titania and silica sources.

Ti(S20)-PMO and Ti(S10)-PMO materials have perfect uniform cylindrical mesopores as evidenced by the type-IV N_2 sorption isotherms with a H1-type hysteresis loop. A type H4 hysteresis loop is observed for Ti(S)-PMO materials with the Si/Ti ratio of 6.7 and 5. Solvent extraction method is applied to remove triblock copolymer in as-made Ti(S)-PMOs. As a result, micropores may be negligible. The *V–t* plot analysis confirms the speculation (Table 1 and SI Fig. S2). Almost undetectable micropores are present in the Ti(S)-PMO materials. Therefore, the H4-type hysteresis loop possibly originates from the narrow slit pores from non-rigid aggregates of plane-like particles [34]. The BET surface area and pore volumes distinctly increase with the decrease in Si/Ti ratio, also possibly due to the formation of narrow slit pores. SEM images (Fig. 5) show the morphology of Ti(S)-PMO materials changes from traditional rods to non-uniform particles and to layered structures when the Si/Ti ratio ranges from 20 to 5. The morphology change may be related to the narrow slit pores.

3.2. Titanium environment

The titanium environment was evaluated by means of FT-IR and diffuse reflectance UV–vis spectroscopy, which are widely used to characterize the framework Ti species in microporous and mesoporous materials, such as TS-1 [35], Ti-MCM-41 [36] and Ti-SBA-15 [37]. The FT-IR spectra for all Ti(M)-SBA materials (Fig. 6a) clearly show strong bands at 3344, 1080, 790 and 960 cm^{-1}. The first three bands could be attributed to the characteristic Si–O–Si vibrations and Si–O–H stretching vibration. Although the presence of a strong band at 960 cm^{-1} cannot be exclusively assigned to the Si–O–Ti stretching vibration, the increasing intensity ratio of I_{960}/I_{790} with the increase of titanium content (from 0.21 to 0.36 wt%) can be regarded as a proof for the incorporation of Ti species into the silica framework [10]. However, this value keeps almost a constant by further increasing titanium content to 1.4 and 1.9 wt% (Si/Ti ratio of 10 and 8.5). At the same

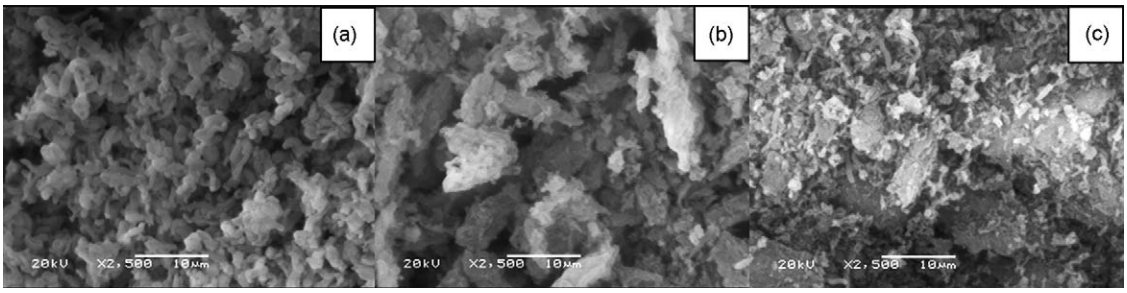

Fig. 5. SEM images of Ti-containing periodic mesoporous organosilicas: Ti(S20)-PMO (a), Ti(S6.7)-PMO (b) and Ti(S5)-PMO (c).

time, anatase appears. These phenomena suggest that redundant titanium cannot co-condense with silica species and intend to aggregate together. The samples with a low titanium content (Ti(M20)-SBA and Ti(M12.5)-SBA) show one strong UV–vis signal located at 210 nm (Fig. 7a), which is attributed to the presence of Ti^{4+} species in a silica matrix adopting a tetrahedral coordination [38]. A weak signal ranging from 250 to 350 nm can also be detected which is usually ascribed to titanium aggregates. The signal becomes strong and dominant when titanium content increases. This phenomenon further indicates that titania aggregate together rather than incorporate into the silica matrix with a high-content titanium. As shown above, the mesostructural regularity is low. In comparison with pure anatase, this signal left shifts, implying that titania aggregates are relatively tiny, in good agreement with the XRD patterns.

When $TiCl_3$ is used as a single inorganic titanium source for the synthesis of Ti(S)-SBA materials, the FT-IR spectra (Fig. 6b) are analogous to those for Ti(M)-SBA, featured by Si–O–Si, Si–OH and Si–O–Ti bands. The fact that the I_{960}/I_{790} ratio increases with the reduction in the Si/Ti ratio (from 20 to 6.7) indicates the incorporation of Ti^{4+} into framework. A high-titanium-content sample (Ti(S5)-SBA) shows no further increase in the I_{960}/I_{790} ratio, reflecting the formation of a large amount of titania. The UV–vis spectra (Fig. 7b) show that the samples Ti(S20)-SBA, Ti(S10)-SBA and Ti(S6.7)-SBA have one strong signal centered at 210 nm and a very weak one at about 260 nm, similar to Ti(M)-SBA with a low titanium content, suggesting the presence of tetrahedrally coordinated Ti species in a silica matrix in the majority. The increase of the titanium content results in appearance of a signal located at about 250 nm, indicating the formation of titania. Similar to Ti(M)-SBA which are prepared with mixed inorganic titanium sources, the content of titanium in Ti(S)-SBA are limited to a certain range. The overmuch titanium would lead to the aggregation of titanium species beyond tetrahedral coordination, and disordered mesostructure.

The FT-IR spectra for Ti(S)-PMO also exhibit characteristic Si–O–Si and Si–O–Ti bands (Fig. 6c). The introduction of titanium into the silica framework is evidenced by the increasing I_{960}/I_{790} ratio by comparing Ti(S20)-PMO and Ti(S10)-PMO with titanium content of 0.21 and 0.33 wt%. For Ti(S6.7)-PMO and Ti(S5)-PMO, the I_{960}/I_{790} ratio almost keeps unchanged despite of the increase in the added amount of $TiCl_3$. This phenomenon is in coincidence with the elemental analysis that reveals the constant titanium content in the Ti(S)-PMO materials with an initial Si/Ti ratio between 10 and 5. Only one strong signal located at 210 nm can be observed in the UV–vis spectra for hybrid Ti(S)-PMO catalysts

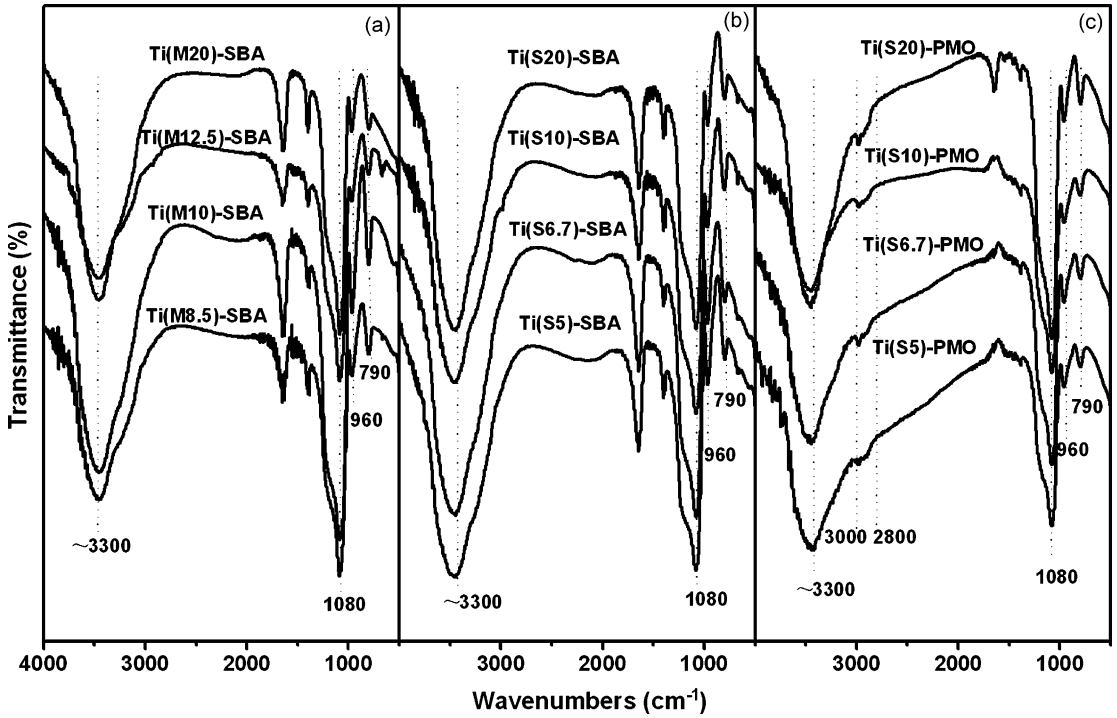

Fig. 6. FT-IR spectra of Ti-containing periodic mesoporous silicas Ti(M)-SBA (a) and Ti(S)-SBA (b) prepared with mixed $TiCl_4$ and TBOT titanium precursors and a single inorganic $TiCl_3$ precursor, respectively, and organosilicas Ti(S)-PMO (c) prepared with a single inorganic $TiCl_3$ precursor.

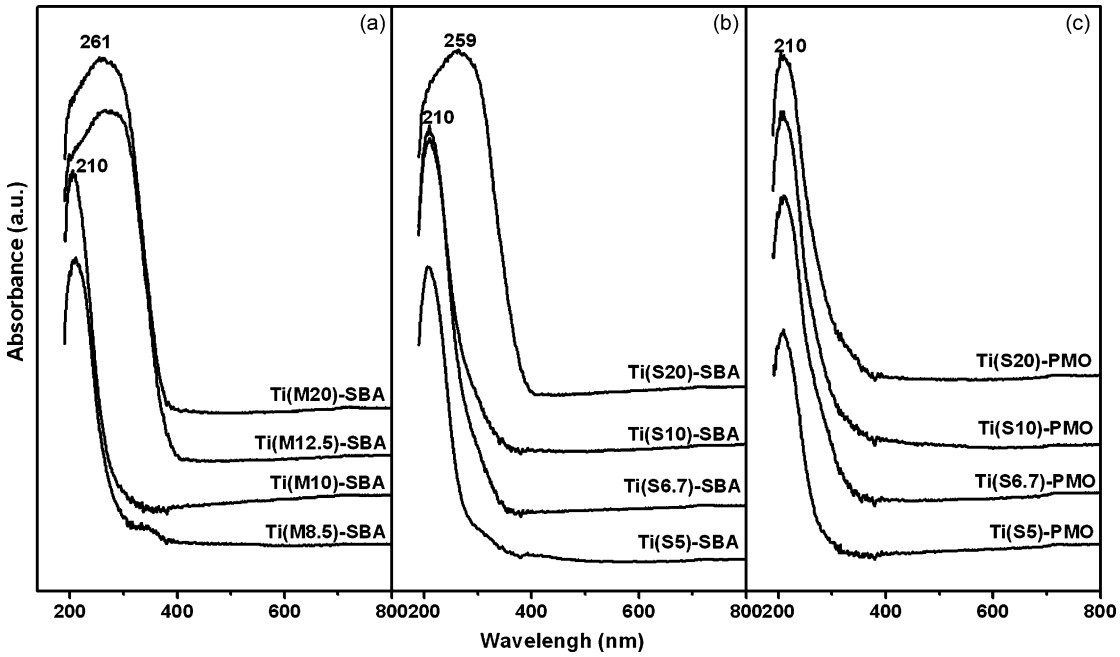

Fig. 7. UV–vis spectra of Ti-containing periodic mesoporous silicas Ti(M)-SBA (a) and Ti(S)-SBA (b) and periodic mesoporous organosilicas Ti(S)-PMO (c).

with a low titanium content (0.21 wt%, Fig. 7c). The signal belonging to titanium aggregate ranging from 250 to 350 nm is very wide and weak even when the Si/Ti ratio reduces to 5, demonstrating the dominant presence of framework titania species.

3.3. Hybrid inorganic–organic framework

Fig. 8 shows the ^{13}C CP MAS-NMR spectrum for Ti(S)-PMO materials after solvent extraction. Three signals at 5, 16 and 58 ppm can be detected. The chemical shift at 5 ppm is unambiguously attributable to bridging ethyl group of the –$SiCH_2CH_2Si$– moieties, suggesting that the integrity of the organic fragment is preserved upon surfactant removal [39]. The latter two signals at 16 and 58 ppm are associated with trace amounts of ethanol used in the extraction process. In addition, the absence of the surfactant resonances located at 30 and 70 ppm after extraction indicates near-complete removal of the surfactant using the acidified ethanol extraction method. The FT-IR spectra (Fig. 6c) show the appearance of absorption bands at 2800–3000 cm^{-1}, assigned to C–H stretching mode from the organic functional groups, confirming the formation of inorganic–organic framework. As far as we know, this is the first report on the synthesis of titanium-containing periodic mesoporous organosilicas by using inorganic titanium solution as titanium source under acidic conditions.

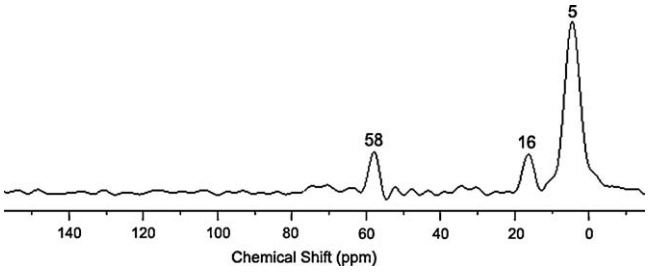

Fig. 8. Solid state ^{13}C CP MAS NMR spectrum for Ti(S10)-PMO prepared by co-condensation of TEOS, BTESE and $TiCl_3$.

4. Conclusion

Titanium-containing ordered mesoporous molecular silicas (Ti-SBA) and organosilicas (Ti-PMO) have been successfully synthesized using inorganic titanium sources via the triblock-copolymer templating co-condensation approach under acidic conditions. The titanium sources can be mixed inorganic "acid–base pairs", namely acidic $TiCl_4$ and basic counterpart $Ti(OC_4H_7)_4$, and a single inorganic $TiCl_3$ precursor. The obtained Ti-containing mesoporous silicas and organosilicas have highly ordered 2D hexagonal structure, uniform pore sizes (5.1–8.0 nm), high surface areas (421–1070 m^2/g), large pore volumes (0.5–1.3 cm^3/g) and tetrahedrally coordinated titanium sites. The decrease of adding Si/Ti ratio causes an increase of titanium content in the silica framework; but the Si/Ti ratio is restricted to a certain range. The maximum titanium content is about 0.34 wt% regardless of the titania and silica sources. The redundant titania sources would aggregate together to form anatase rather than incorporate into silica framework, accompanying the loss of mesostructural regularity.

Acknowledgments

This work was financially supported by the Shell Co. We thank Dr. Jan Karel Buijink and Dr. Cristina Nenu from Shell Co for the fruitful discussion. Y.W. thanks the funding of 07QH14011, 07SG49, and NCET-07-0560 for supporting the research.

Appendix A. Supplementary data

Supplementary data associated with this article can be found, in the online version, at doi:10.1016/j.cattod.2009.03.008.

References

[1] C.T. Kresge, M.E. Leonowicz, W.J. Roth, J.C. Vartuli, J.S. Beck, Nature 359 (1992) 710.
[2] J.S. Beck, J.C. Vartuli, W.J. Roth, M.E. Leonowicz, C.T. Kresge, K.D. Schmitt, C.T.W. Chu, D.H. Olson, E.W. Sheppard, S.B. McCullen, J.B. Higgins, J.L. Schlenker, J. Am. Chem. Soc. 114 (1992) 10834.
[3] D.Y. Zhao, Q.H. Huo, J.L. Feng, B.F. Chmelka, G.D. Stucky, J. Am. Chem. Soc. 120 (1998) 6024.
[4] M.S. Morey, S. O'Brien, S. Schwarz, G.D. Stucky, Chem. Mater. 12 (2000) 898.
[5] J.Q. Yu, C. Li, L. Xu, M.J. Li, Q. Xin, Z.M. Liu, Chin. J. Catal. 22 (2001) 267.

[6] D. Ji, T. Ren, L. Yan, J.S. Suo, Mater. Lett. 57 (2003) 4474.
[7] B.L. Newalkar, J. Olanrewaju, S. Komarneni, Chem. Mater. 13 (2001) 552.
[8] Z.H. Luan, L. Kevan, Micropor. Mesopor. Mater. 44 (2001) 337.
[9] T.E.W. Niessen, J.P.M. Niederer, T. Gjervan, W.F. Holderich, Micropor. Mesopor. Mater. 21 (1998) 67.
[10] R. Ryoo, C.H. Ko, R.F. Howe, Chem. Mat. 9 (1997) 1607.
[11] W.H. Zhang, M. Froba, J.L. Wang, P.T. Tanev, J. Wong, T.J. Pinnavaia, J. Am. Chem. Soc. 118 (1996) 9164.
[12] W.H. Zhang, J.Q. Lu, B. Han, M.J. Li, J.H. Xiu, P.L. Ying, C. Li, Chem. Mat. 14 (2002) 3413.
[13] J.A. Melero, J.M. Arsuaga, P.G. de Frutos, J. Iglesias, J. Sainz, S. Blazquez, Micropor. Mesopor. Mater. 86 (2005) 364.
[14] Y. Wan, H.F. Yang, D.Y. Zhao, Acc. Chem. Res. 39 (2006) 423.
[15] S.D. Shen, Y. Deng, G.B. Zhu, D.S. Mao, Y.H. Wang, G.S. Wu, J. Li, X.Z. Liu, G.Z. Lu, D.Y. Zhao, J. Mater. Sci. 42 (2007) 7057.
[16] P.T. Tanev, M. Chibwe, T.J. Pinnavaia, Nature 368 (1994) 321.
[17] S. Gontier, A. Tuel, Zeolites 15 (1995) 601.
[18] W. Cho, J.W. Park, C.S. Ha, Mater. Lett. 58 (2004) 3551.
[19] J. Pires, M. Pinto, J. Estella, J.C. Echeverria, J. Colloid Interface Sci. 317 (2008) 206.
[20] Q. Gao, W.J. Xu, Y. Xu, D. Wu, Y.H. Sun, F. Deng, W.L. Shen, J. Phys Chem. B 112 (2008) 2261.
[21] M.C. Capel-Sanchez, L. Barrio, J.M. Campos-Martin, J.L.G. Fierro, J. Colloid Interface Sci. 277 (2004) 146.
[22] M.P. Kapoor, A.K. Sinha, S. Seelan, S. Inagaki, S. Tsubota, H. Yoshida, M. Haruta, Chem. Commun. (2002) 2902.
[23] B.Z. Tian, X.Y. Liu, B. Tu, C.Z. Yu, J. Fan, L.M. Wang, S.H. Xie, G.D. Stucky, D.Y. Zhao, Nature Mater. 2 (2003) 159.
[24] N.N. Trukhan, A.A. Panchenko, E. Roduner, M.S. Mel'gunov, O.A. Kholdeeva, J. Mrowiec-Bialon, A.B. Jarzebski, Langmuir 21 (2005) 10545.
[25] Y. Wan, H.X. Ma, Z. Wang, W. Zhou, Micropor. Mesopor. Mater. 76 (2004) 35.
[26] T. Matthias, E.J. Cejka, A. Corma, F. Schueth, Stud. Surf. Sci. Catal. 168 (2007) 495.
[27] B.Z. Tian, H.F. Yang, X.Y. Liu, S.H. Xie, C.Z. Yu, J. Fan, B. Tu, D.Y. Zhao, Chem. Commun. (2002) 1824.
[28] Y. Wan, D.Y. Zhao, Chem. Rev. 107 (2007) 2821.
[29] Y. Wan, Y.F. Shi, D.Y. Zhao, Chem. Commun. (2007) 897.
[30] A.S.M. Chong, X.S. Zhao, J. Phys. Chem. B 107 (2003) 12650.
[31] S. Inagaki, S. Guan, Y. Fukushima, T. Ohsuna, O. Terasaki, J. Am. Chem. Soc. 121 (1999) 9611.
[32] T. Asefa, M.J. MacLachan, N. Coombs, G.A. Ozin, Nature 402 (1999) 867.
[33] B.J. Melde, B.T. Holland, C.F. Blanford, A. Stein, Chem. Mater. 11 (1999) 3302.
[34] T. Matthias, in: J. Cejka, H. van Bekkum, A. Corma, F. Schueth (Eds.), Introduction to Zeolite Science and Practice, Studies in Surface Science and Catalysis, vol. 168, 2007, p. 495.
[35] Y. Liu, L. Zong, F. Xin, Mater. Res. Innov. 12 (2008) 84.
[36] E. Gianotti, V. Dellarocca, L. Marchese, G. Martra, S. Coluccia, T. Maschmeyer, Phys. Chem. Chem. Phys. 4 (2002) 6109.
[37] G. Li, X.S. Zhao, Ind. Eng. Chem. Res. 45 (2006) 3569.
[38] G.N. Vayssilov, Z. Popova, A. Tuel, Chem. Eng. Technol. 20 (1997) 333.
[39] U. Diaz-Morales, G. Bellussi, A. Carati, R. Millini, W.O. Parker, C. Rizzo, Micropor. Mesopor. Mater. 87 (2006) 185.